JVI Journals.ASM.org

Retroviral Cyclin Enhances Cyclin-Dependent Kinase-8 Activity

Joel Rovnak, Connie D. Brewster, and Sandra L. Quackenbush

Department of Microbiology, Immunology, and Pathology, Colorado State University, Fort Collins, Colorado, USA

Alterations in the functional levels of cyclin-dependent kinase-8 (CDK8) or its partner, cyclin C, have been clearly associated with cancers, including colon cancer, melanoma, and osteosarcoma. Walleye dermal sarcoma virus encodes a retroviral cyclin (RV-cyclin) that localizes to interchromatin granule clusters and binds CDK8. It also binds to the Aα subunit (PR65) of protein phosphatase 2A (PP2A). Binding to the Aα subunit excludes the regulatory B subunit, but not the catalytic C subunit, in a manner similar to that of T antigens of the small DNA tumor viruses. The expression of the RV-cyclin enhances the activity of immune affinity-purified CDK8 *in vitro* for RNA polymerase II carboxy-terminal domain (CTD) and histone H3 substrates. PP2A also enhances CDK8 kinase activity *in vitro* for the CTD but not for histone H3. The PP2A enhancement of CDK8 is independent of RV-cyclin expression and likely plays a role in the normal regulation of CDK8. The manipulation of endogenous PP2A activity by inhibition, amendment, or depletion confirmed its role in CDK8 activation by triggering CDK8 autophosphorylation. Although RV-cyclin and PP2A both enhance CDK8 activity, their actions are uncoupled and additive in kinase reactions. PP2A may be recruited to CDK8 in the Mediator complex by a specific PP2A B subunit or additionally by the RV-cyclin in infected cells, but the RV-cyclin appears to activate CDK8 directly and in a manner independent of its physical association with PP2A.

The complex retrovirus walleye dermal sarcoma virus (WDSV) is associated with a neoplastic disease that develops and regresses seasonally (6, 7, 31, 32, 39, 58). During the development of dermal sarcoma, only two viral transcripts are expressed, and they encode the accessory proteins retroviral cyclin (RV-cyclin) and Orf B, suggesting the involvement of these proteins in tumorigenesis (8, 32, 39, 43).

RV-cyclin is predominantly nuclear, is concentrated in interchromatin granule clusters (IGCs; also called nuclear speckles), and copurifies with components of the transcription machinery (43, 46). RV-cyclin directly inhibits transcription at the WDSV promoter and at NF-κB- and interferon-dependent promoters in mammalian and piscine cells (40, 46, 60), but RV-cyclin also significantly enhances transcript levels from select cell cycle-regulatory genes (9). RV-cyclin contains two known functional domains, a transcription activation domain (AD) and a cyclin box fold (29, 40, 45, 47). The AD is located near the carboxy terminus and directly contacts TATA binding protein-associated factor 9 (TAF9) in mammalian and piscine cells (45). Mutations within the AD that disrupt TAF9 binding also interfere with RV-cyclin's function in transcription (45, 47). The majority of the RV-cyclin structure is comprised of a cyclin box fold, which is responsible for binding to cyclin-dependent kinase-8 (CDK8) (9, 29, 46). CDK8, cyclin C, and Mediator proteins Med12 and Med13 comprise the CDK8 submodule of the Mediator complex. The Mediator complex consists of a set of 26 highly conserved proteins that function to support transcription through its interactions with general transcription factors or specific DNA-binding transcription factors and the large subunit of RNA polymerase II (RNA Pol II) (11, 17). Known substrates for CDK8 phosphorylation include the carboxy-terminal domain (CTD) of RNA Pol II, E2F1, SMAD, cyclin H, histone H3, and Med13 (1, 2, 4, 27, 33, 34, 41, 42). CDK8 is also subject to autophosphorylation, and this event is associated with kinase activation (19, 26).

A loss-of-function screen for genes that regulate β-catenin transcriptional activity in human colon cancer cells identified CDK8 as an oncogene (16). Morris et al. (34) demonstrated that phosphorylation by CDK8 inactivates E2F1, resulting in enhanced β-catenin transcriptional activity. CDK8 is located in a region of chromosome 13 that is frequently amplified in colon cancer (16, 30, 54). This amplification was also observed in colon cancer cell lines, and the knockdown of CDK8 expression can reverse the growth of these lines. The overexpression of CDK8 is also able to transform NIH 3T3 cells (16). A kinase-deficient CDK8 mutant (D173A) does not transform cells, indicating a requirement for kinase activity in transformation and the maintenance of the transformed phenotype.

Mechanisms for the regulation of CDK8 activity are currently unclear. Interactions with both cyclin C and Med12 have been shown to be required for activity by recombinant CDK8 (26), and autophosphorylation is required for full activation (19). Two phosphorylation sites have been confirmed by analyses of the phosphoproteome of HeLa cells, T410 and S413 (36), but such studies were not comprehensive in regard to the identification of possible CDK8 phosphoepitopes and do not identify the responsible kinase. CDK8 lacks a residue for phosphorylation in its T loop, making it unique among CDKs for activation at this motif (23, 50). It is proposed that a glutamate in cyclin C mimics a phosphoresidue that interacts with three conserved arginines within the loop (23, 50). Interaction with Med12 may be required for CDK8 activation to initiate conformational changes that alter the ATP binding site (26, 50). Further studies are needed to decipher the mechanisms that regulate CDK8 kinase activity.

Protein stability, localization, and function are frequently regulated by phosphorylation. Protein phosphatase 2A (PP2A) is one

Received 5 December 2011 Accepted 23 February 2012

Published ahead of print 29 February 2012

Address correspondence to Sandra L. Quackenbush, sandra.quackenbush@colostate.edu.

doi:10.1128/JVI.07006-11

of four major serine/threonine phosphatases in the cell, and it functions in the negative control of cell growth and division (10, 49). PP2A is a multimeric enzyme comprised of a catalytic C subunit (PP2A C), a scaffold A subunit (Aα or Aβ; PR65), and a regulatory B subunit. There are four B subunit families, which generate a large variety of PP2A holoenzymes with varied localization and substrate recognition. Simian virus 40 (SV40) small t and polyomavirus small t and middle T antigens can displace the B regulatory subunit from the PP2A core enzyme and subvert PP2A activity (37, 38, 52, 55). The transformation of 3T3 cells by polyoma middle T antigen is dependent upon this interaction with PP2A.

An interaction between the RV-cyclin of WDSV and the Aα subunit, PR65, of PP2A was detected in a yeast two-hybrid screen, and in cell culture RV-cyclin associates preferentially with the A and C core enzymes of PP2A without the B subunit. In kinase assays that assess RV-cyclin's effects on CDK8 activity, a PP2A inhibitor, okadaic acid (OA), was incorporated to exclude PP2A activity and protect newly labeled substrates. Rather than protecting signal, OA reduced the apparent kinase activity. Herein we demonstrate not only the enhancement of CDK8 activity by RV-cyclin but also the positive regulation of CDK8 activity by PP2A whether or not RV-cyclin is present. A dephosphorylation event leads to CDK8 autophosphorylation and full activation *in vitro*. The activating phosphatase was made apparent by the retroviral cyclin, and we hypothesize that RV-cyclin recruits PP2A to CDK8. However, the RV-cyclin enhancement of CDK8 is additive to PP2A enhancement, suggesting a separate and more direct mechanism for RV-cyclin action.

MATERIALS AND METHODS

Yeast two-hybrid screen. WDSV RV-cyclin sequences were derived from the pKH3OrfA construct by PCR amplification using 5′ and 3′ primers that incorporate EcoRI and BamHI restriction sites, respectively (43, 45). The amplified products were digested and ligated into the GAL4 DNA binding domain vector pAS2-1 and used as bait to screen a pACT2 GAL4 AD fusion HeLa cDNA library (Matchmaker GAL4 two-hybrid system; Clontech). *Saccharomyces cerevisiae* strain Y190 was cotransformed with the bait plasmid pAS2-1-RV-cyclin$_{1\text{-}219}$ or pAS2-1-RV-cyclin$_{112\text{-}297}$ and the pACT2 cDNA library. Positive clones were initially selected based on the ability to grow in the absence of histidine, leucine, and tryptophan but in the presence of 25 mM 3-amino 1,2,4-triazole (3-AT). Positive colonies were further screened for β-galactosidase activity by a colony lift assay according to the manufacturer's instructions (Clontech). Plasmid DNA was isolated from clones positive for β-galactosidase activity and sequenced.

Cells and protein expression. The larger pACT2 GAL4 AD-PR65 cDNA insert (amino acids [aa] 212 to 568), isolated from the yeast two-hybrid screen, was subcloned into pCMV-myc (Clontech) at EcoRI and XhoI sites. pCMV-myc contains a cytomegalovirus (CMV) promoter and fuses a myc epitope tag onto the amino terminus of the expressed protein. Glutathione *S*-transferase (GST)-CTD, pFLAG-CDK8, and pKH3-RV-cyclin and pKH3-cyclin C vectors were described previously, as well as HeLa Tet-Off cells (BD Biosciences), with myc-tagged RV-cyclin induction in the absence of doxycycline (9). Kinase-deficient pFLAG-CDK8 (D173A) was prepared by the site-directed mutagenesis of pFLAG-CDK8. HeLa cells were maintained in Dulbecco's modified Eagle medium with 10% fetal bovine sera and 4 mM glutamine at 37°C in 5% CO_2. Transient transfections were performed with Fugene 6 according to the manufacturer's instructions (Roche). For the precipitation of HA-RV-cyclin and myc-tagged or endogenous PR65, cells were lysed at 48 h posttransfection in immunoprecipitation (IP) buffer (1% Triton X-100, 0.5% NP-40, 150 mM NaCl, 10 mM Tris-HCl [pH 7.5], 1 mM EDTA, 1 mM EGTA) with protease and phosphatase inhibitors (2 μg/ml leupeptin and aprotinin, 1 μg/ml pepstatin, 0.2 mM phenylmethylsulfonyl fluoride [PMSF], 0.2 mM sodium orthovanadate, 2 mM sodium pyrophosphate, and 1 mM glycerophosphate). Lysates were precleared with 1 μg normal rabbit serum and 50 μl protein G Sepharose (50:50) per mg total protein, and 100-μg equivalents at 1 μg/μl were incubated with 0.5 to 1.0 μg mouse anti-HA (clone 12CA5; Roche), anti-myc (clone 9E10; Santa Cruz), anti-PP2A-Aα (clone 5H4, 6G3, or 6F9; Covance), or goat anti-PR65 (PP2A-Aα/β [C-20]; sc-6112; Santa Cruz) and 30 μl protein G Sepharose suspension (50:50) overnight at 4°C. Protein G pellets were washed 4 times with IP buffer, and bound proteins were separated on polyacrylamide gels. Western blots were probed with anti-hemagglutinin (HA), anti-myc, or goat anti-PR65. Five μg of protein from cell lysates was loaded in control lanes.

Preparation of NEs. Nuclear extracts (NEs) were prepared as previously described (9), except with the exclusion of phosphatase inhibitors. Briefly, nuclei were isolated after cell lysis in 0.5% NP-40 in phosphate-buffered saline (PBS) (6) and then washed three times in PBS and once in buffer A (10 mM HEPES, pH 8.0, 10 mM KCl, 1.5 mM $MgCl_2$, 0.5 mM dithiothreitol [DTT]) prior to salt extraction by suspension in 2.5× packed nuclear volume of buffer C (12) (10 mM HEPES, pH 8.0, 420 mM KCl, 20% glycerol, 0.1 mM EDTA, 0.5 mM DTT, and protease inhibitors) for 1 h at 4°C. Extracts were clarified at 21,000 × *g* for 20 min and precleared with 1 μg each normal rabbit and goat serum and 100 μl protein G Sepharose suspension (50:50) overnight at 4°C in buffer C without glycerol and with 0.05% NP-40.

Kinase assays. Twenty μg precleared nuclear extracts (40 μl) were incubated overnight with 0.25 to 1 μg specific antibody (Ab) and 8 μl protein G magnetic beads (Dynabeads; Invitrogen). Antibodies included mouse anti-cdk7/CAK (MO-1.1; Sigma), goat anti-cdk8 (C-19; sc-1521; Santa Cruz), goat anti-cdk9 (C-20; sc-484; Santa Cruz), and goat anti-PR65 (PP2A-A/β [C-20]; sc-6112; Santa Cruz). For dual precipitations, the quantity of Dynabeads was doubled. For triplicate kinase samples, 3-fold amounts of nuclear extract were subject to IP with 3-fold quantities of antibodies and magnetic beads. Beads were washed four times with buffer C (without glycerol and with 0.05% NP-40) and two times with kinase buffer (50 mM Tris-HCl, pH 7.5, 10 mM $MgCl_2$, 0.1 mM EDTA, 0.05 mM DTT) with 0.05% NP-40. Triplicate kinase samples were split into three equal aliquots of suspended beads in the final wash. Individual kinase reactions (20 μl) contained 1 μg of GST-CTD or purified mouse histone H3 (a generous gift from Teri McLain, Department of Biochemistry and Molecular Biology, Colorado State University, Fort Collins, CO) and 0.25 to 0.5 μCi [γ-^{32}P]ATP (6,000 Ci/mmol; Perkin Elmer) in kinase buffer. Master mixes containing all components were split for the inclusion of OA (1 to 100 nM) and dispensed to protein G beads. Reaction mixtures were mixed at setting 1 on a vortexer for 50 min at 30°C, supplemented with 5 μl of glutathione magnetic beads, and mixed for 15 min at room temperature to capture GST-CTD substrate. All reactants, bound to either protein G or glutathione beads, were washed three times with kinase buffer with 0.05% NP-40 prior to the suspension of beads in loading dye and separation on polyacrylamide gels and Western blotting. In the case of histone H3, substrate was captured with 0.5 μg rabbit anti-histone H3 (9715; Cell Signaling) and 5 μl additional protein G beads. Western blots were dried in methanol and exposed to phosphor screens for image capture on a Bio-Rad molecular imager FX. Multiple exposures were made to ensure images in the linear response range of the screens. Lane and band selection and densitometry of individual bands was performed directly on Quantity One software (Bio-Rad) image files using Image Lab 3.0 software (Bio-Rad) to yield relative band volume. These values correlated with total counts per band as determined with Quantity One software. Averages and standard deviations were determined with Excel software (Microsoft). Student's *t* test (see Fig. 1 and 6) and 95% confidence intervals based on a *t* distribution or two-way analysis of variance (see Fig. 3 and 7) were used for the analysis of data. A *P* value of less than 0.05 was considered significant. Results directly comparing NEs are from the same exposure time (except where indicated) and from matched

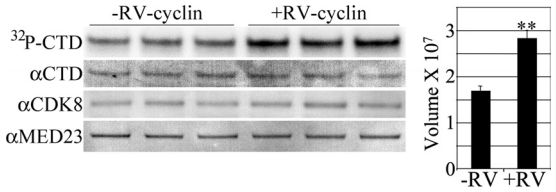

FIG 1 RV-cyclin enhancement of CDK8 activity. Anti-CDK8 IPs from nuclear extracts of matched uninduced (−RV-cyclin) and induced (+RV-cyclin) HeLa cells were assayed in triplicate reactions. Equal aliquots of washed CDK8 Ab-protein G magnetic beads were suspended in a common reaction mix. After incubation, GST fusion substrate was captured with added glutathione magnetic beads. IP and substrate were washed and separated by polyacrylamide gel electrophoresis and blotted onto nylon for the imaging of labeled GST-CTD substrate (^{32}P-CTD). The blot was subsequently probed with specific antibodies for GST-CTD (74 to 76 kDa; αCTD), CDK8 (53 kDa; αCDK8), and MED23 (140 kDa; αMED23). The chart presents means and standard deviations of signal (relative band volume) from the phosphorimage of the CTD band. Asterisks indicate the statistical significance of the increase associated with RV-cyclin expression ($P < 0.001$).

kinase reactions performed at the same time using the same reaction mix. After image capture, blots were rewet in methanol, rehydrated, and blocked in 5% milk. GST-CTD was detected with monoclonal antibody (MAb) reactive to RNAPII CTD (clone 8WG16; Covance). Additional antibodies included anti-CDK7, anti-CDK8, anti-CDK9 (see above), anti-MED23 (anti-SUR-2; clone D27-1805; BD Biosciences), and rabbit anti-histone H3. Primary antibodies were detected with appropriate secondary antibody-peroxidase conjugates and TMB colorimetric substrate (KPL). Antibody complexes were removed from blots by incubation for 1 h at 50°C in Western strip buffer (62 mM Tris-HCl [pH 6.8], 2% SDS, and 100 mM β-mercaptoethanol) prior to probing with successive antibodies. Western blots were captured on a Visioneer 9420 reflective scanner with Photoshop CS 8.0 (Adobe). Composite images were assembled and levels of all parts of each panel adjusted at once with Photoshop CS5 extended version 12.0 ×32.

RESULTS

RV-cyclin enhances CDK8 kinase activity *in vitro*. We previously showed that RV-cyclin binds CDK8 (9). To assess the effect of RV-cyclin on CDK8 kinase activity, CDK8 was immunoprecipitated (IP) with anti-CDK8 antibody from nuclear extracts of HeLa cells with or without induced RV-cyclin expression (Tet-off induction). IPs on protein G magnetic beads were assayed *in vitro* with [γ-^{32}P]ATP and a GST-CTD fusion protein as substrates. Labeled GST-CTD was captured by the addition of glutathione magnetic beads after the reaction. Bound IP and substrate were then washed and separated by gel electrophoresis under denaturing conditions. The gels were blotted onto nylon membranes for radiography (phosphorimaging) and subsequent Western analysis. The induction of RV-cyclin expression yielded a 40% increase in CDK8 activity in IPs from equivalent amounts of nuclear extract (20 μg) (Fig. 1). After imaging, blots were probed successively with antibodies for GST-CTD, CDK8, and MED23 (Mediator component) to demonstrate equivalent substrate and enzyme input and the coimmunoprecipitation (co-IP) of the Mediator complex with anti-CDK8 Ab. There was no significant increase in CDK8 mRNA expression as determined by quantitative reverse transcription-PCR (not shown) or by Western blotting (Fig. 1) after the induction of RV-cyclin. These assays were run in the presence of excess okadaic acid (100 nM) to protect newly radiolabeled substrate from any phosphatase activity that might be present in the IPs.

WDSV RV-cyclin interacts with the Aα subunit of PP2A. A yeast two-hybrid screen was used to identify cellular proteins that interact with WDSV RV-cyclin. Our previous work showed that a fusion of full-length RV-cyclin to the GAL4 DNA binding domain (pAS2-1-RV-cyclin$_{1\text{-}297}$) autonomously activated the *lacZ* reporter gene (45). The deletion of either the N-terminal 112 amino acids (pAS2-1-RV-cyclin$_{112\text{-}297}$) or C-terminal 78 amino acids (pAS2-1-RV-cyclin$_{1\text{-}219}$) yielded constructs negative for autonomous activation (45), allowing the separate representation of the entire RV-cyclin protein in two-hybrid screens of a HeLa cDNA library. Of 16 β-galactosidase-positive clones, 2 contained partial cDNAs of the regulatory Aα subunit of PP2A, PR65. The PR65 clones were isolated independently with amino- and carboxy-truncated RV-cyclin constructs, delimiting the region between amino acids 112 and 219 for PR65 interaction. This region lies within the predicted cyclin box fold of the RV-cyclin (amino acids 17 to 231). The two PR65 clones encode amino acids 212 to 568 and 298 to 568, identifying amino acids 298 to 568 as sufficient for RV-cyclin interaction. This region includes complete HEAT repeat regions 9 to 14 of PR65 (of 15 total). HEAT repeats, named for Huntingtin, elongation factor 3, A subunit of PP2A, and TOR1, are tandemly repeated, 37- to 47-amino-acid modules that form a rod-like scaffold for protein-protein interaction. In PR65, 38-amino-acid repeats consist of pairs of anti-parallel α helices (21). Repeats 1 to 10 (amino acids 8 to 397) bind the B subunit, and repeats 13 to 15 (475 to 589) bind the catalytic subunit (48). The two-hybrid data delimit binding, via sequence in the cyclin box fold of RV-cyclin, to some or all of PR65 HEAT repeats 9 to 14. These repeats overlap the regions that bind B and C subunits by one and two repeats, respectively. These PR65 sequences are highly conserved in eukaryotic organisms. For example, zebrafish PR65 Aα (*Danio rerio*) is 95% identical to human PR65 Aα in the region containing HEAT repeats 9 to 12.

The interaction of RV-cyclin with PP2A was first confirmed by co-IP. The PR65 cDNA clone corresponding to aa 212 to 568 was subcloned into the pCMV-myc vector (pCMV-myc PP2A), and lysates from HeLa cells expressing myc-tagged PR65$_{212\text{-}568}$ and HA-tagged RV-cyclin$_{1\text{-}297}$ were precipitated with anti-myc or anti-HA. Co-IPs were observed on Western blots with antibodies to the respective tags to confirm the interaction of the overexpressed proteins (Fig. 2A).

WDSV RV-cyclin interacts with the PP2A core enzyme. The PP2A core enzyme consists of the catalytic subunit on the PR65 scaffold. The binding of the B subunit to the core enzyme results in the formation of the PP2A holoenzyme. Diversity in PP2A substrate recognition and subcellular localization is dependent on B subunit diversity. Kremmer et al. (28) developed monoclonal antibodies that are reactive to the N terminus of PR65 (MAb clone 6F9), the N-terminal region in HEAT repeat 1 (MAb clone 5H4), and the carboxy terminus (MAb clone 6G3). 6F9 binds to the PP2A holoenzyme (A, B, and C subunits); the binding of 5H4 is occluded by the B subunit, so it binds only the A and C core enzyme; 6G3 is occluded by the C subunit, and it identifies free PR65. The binding of the C subunit is necessary for the cooperative binding of the B subunit (28). Lysates of HeLa cells transfected with a vector expressing HA-RV-cyclin or control vector were subject to IP with these antibodies or with polyclonal anti-PR65 to characterize RV-cyclin association with the PP2A enzyme (Fig. 2B). RV-cyclin interacts primarily with the core enzyme (5H4; A and C subunits) rather than with free PR65 or PR65 in the PP2A holoenzyme. This result indicates that the B subunit is not present

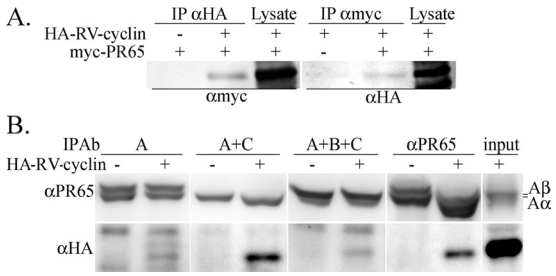

FIG 2 WDSV RV-cyclin interacts with PP2A. (A) Lysates of HeLa cells transfected with constructs expressing myc-tagged PR65 (aa 212 to 568; 40 kDa; myc-PR65) and HA-tagged RV-cyclin (37 kDa; HA-RV-cyclin) were subject to IP with anti-HA (αHA) and anti-myc (αmyc) antibodies, and Western blots were probed with the reciprocal antibodies. Lysate lanes contain 10 μg cell lysate. (B) Co-IP of expressed HA-RV-cyclin with endogenous PR65. Lysate from HeLa cells transfected with control vector or HA-RV-cyclin expression vector were subjected to IP with monoclonal antibodies that distinguish free PR65 Aα and Aβ subunits of PP2A (65 kDa; 6G3; A), the PP2A core enzyme (5H4; A+C), or the PP2A holoenzyme (6F9; A+B+C) and with polyclonal anti-PR65 Aα/β that precipitates all forms (αPR65). The input lane contains 10 μg lysate.

when RV-cyclin binds. This is in common with the DNA tumor virus antigens, SV40 small t and polyoma small t and middle T. However, the binding of RV-cyclin within PR65 repeats 9 to 14 distinguishes it from the DNA tumor virus antigens whose sites of interaction reside in repeats 2 to 8 of PR65 (48). It is not clear why there is reduced signal with the 6F9 holoenzyme antibody, which should detect the RV-cyclin-A-C heterotrimer, but it suggests interference with 6F9 at the N terminus when RV-cyclin is present.

CDK8 kinase activity is regulated by PP2A. To determine whether PP2A activity affects the signal in the CDK8 kinase assay, equal aliquots of anti-CDK8-IP bead suspensions were tested in the same reaction mix but with or without OA (Fig. 3A). IPs from nuclear extracts of cells with or without induced RV-cyclin expression were included. Rather than losing signal to phosphatase activity, the apparent CTD phosphorylation was significantly increased without OA in the reaction. This outcome was the same whether or not RV-cyclin was expressed. Sixty-four percent of the CDK8 activity was lost when 10 nM OA was included in the kinase reaction of nuclear extracts from cells without RV-cyclin (Fig. 3A, graph, compare lanes 1 and 2; $P < 0.001$). These results suggest the activation of CDK8 by an OA-sensitive phosphatase that is coprecipitated with CDK8. When OA was included in the kinase reaction of nuclear extracts from cells with RV-cyclin, there was a loss of only 36% of the CDK8 activity (Fig. 3A, graph, compare lanes 3 and 4; $P < 0.01$). In the absence of OA, an increase in CDK8 activity was observed in nuclear extracts from RV-cyclin-expressing cells, although the enhanced activity was not significant (Fig. 3A, graph, compare lanes 2 and 4). The same OA inhibition of CDK8 activity was observed with anti-CDK8 IPs from nuclear extracts from the RV-cyclin-positive walleye tumor cell line STEC (44) (Fig. 3B). In these kinase reactions, there was a loss of 35% of CDK8 activity when OA was included. Collectively, these data indicate a function for RV-cyclin that is independent of an OA-sensitive phosphatase for the enhancement of CDK8 activity.

Phosphatases PP2A and PP1 are both sensitive to inhibition by OA, but PP2A is most sensitive, with 50% inhibitory concentrations (IC_{50}s) of 0.5 to 1 nM (24). PP1 is inhibited at higher con-

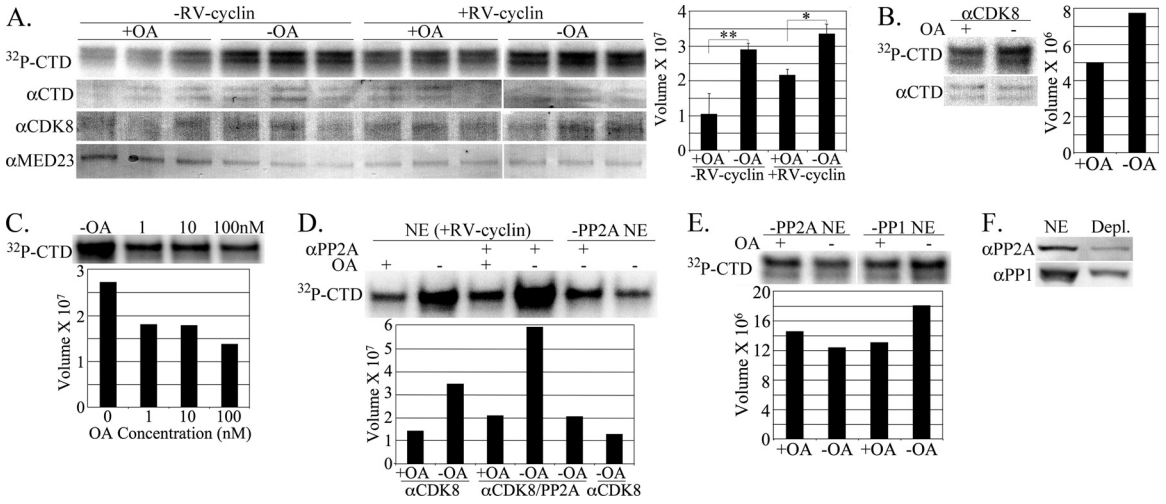

FIG 3 Okadaic acid (OA) inhibits CDK8 kinase activity. (A) Anti-CDK8 IPs from nuclear extracts of matched uninduced (−RV-cyclin) and induced (+RV-cyclin) HeLa cells were assayed in triplicate reactions. Equal aliquots of washed CDK8 Ab-protein G magnetic beads were suspended in a common reaction mix with or without added OA (10 nM). After incubation, GST fusion substrate was captured with added glutathione magnetic beads. IP and substrate were washed and separated by polyacrylamide gel electrophoresis and blotted onto nylon for the imaging of labeled GST-CTD substrate (^{32}P-CTD). The blot was subsequently probed with specific antibodies for the GST-CTD (74 to 76 kDa; αCTD), CDK8 (53 kDa; αCDK8), and MED23 (140 kDa; αMED23). The chart presents means and standard deviations of signal (relative band volume) from the phosphorimage of the CTD band. Statistical significance is represented by asterisks (*, $P < 0.01$; **, $P < 0.001$). These data are representative of three independent experiments. (B) Assay of anti-CDK8 IPs from nuclear extracts of walleye cells with and without the inclusion of OA (10 nM) in the reaction mix. (C) Titration of OA in kinase assay of anti-CDK8 IPs from RV-cyclin-positive HeLa cell nuclear extract. Equal aliquots of washed CDK8 Ab-protein G magnetic beads were suspended in a common reaction mix with or without added OA as indicated. (D) Assay of anti-CDK8 and combined anti-CDK8/anti-PP2A IPs from RV-cyclin-positive HeLa cell nuclear extract [NE (+RV-cyclin)] or the same extract immune depleted of PP2A (−PP2A NE) in a common reaction mix with or without added OA (10 nM). (E) Assay of anti-CDK8 IPs from RV-cyclin-positive HeLa cell nuclear extracts previously immune depleted of PP2A (−PP2A NE) or PP1 (−PP1 NE) with or without added OA (10 nM). Charts present signal (relative band volume) from the phosphorimage of the CTD band in each experiment. (F) Western blot evaluation of depleted (Depl.) nuclear extracts. Ten μg total protein was probed for PR65 (65 kDa; αPR65) and PP1 (34 kDa; αPP1) before and after immune depletion.

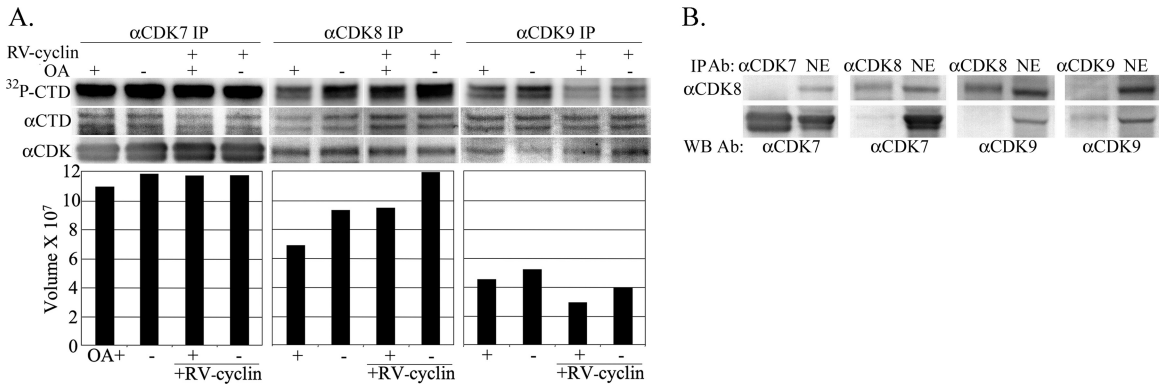

FIG 4 RV-cyclin only enhances CDK8 activity. (A) Anti-CDK7, anti-CDK8, and anti-CDK9 IPs from nuclear extracts of matched uninduced and induced (RV-cyclin +) HeLa cells were assayed for kinase activity with the GST-CTD substrate. Equal aliquots of washed Ab-protein G magnetic beads were suspended in a common reaction mix with or without added OA (10 nM). After incubation, GST fusion substrate was captured with added glutathione magnetic beads. IP and substrate were washed and separated by polyacrylamide gel electrophoresis and blotted onto nylon for the imaging of labeled GST-CTD substrate (^{32}P-CTD). Blots were subsequently probed with specific antibodies for the CTD (74 to 76 kDa; αCTD) and the corresponding IP Ab (first panel, αCDK7, 40 to 42 kDa; second panel, αCDK8, 53 kDa; third panel, αCDK9, 42 kDa). Image exposures were 30 min for CDK7 IPs and 3 h for CDK8 and CDK9 IPs. The charts present signal (relative band volume) from the phosphorimage of the CTD band. (B) Coprecipitation of CDKs. Western blots of CDK IPs (αCDK7, αCDK8, or αCDK9) and 10 μg HeLa nuclear extract (NE) were probed for CDK8 (αCDK8; upper panels) and for CDK7 and CDK9 (αCDK7 or αCDK9; lower panels).

centrations (IC_{50} of 60 to 500 nM). The titration of OA in reactions with four matched aliquots of CDK8-IP bead suspensions demonstrated a loss of 34% of CDK8 activity at 1 nM (Fig. 3C). Only PP2A is effectively inhibited at this OA concentration.

Anti-PP2A antibody (anti-PR65α/β) was included with anti-CDK8 antibody in the same IP to directly test PP2A in the activation of CDK8. The inclusion of PP2A increased the CDK8 activity by 41% compared to that with anti-CDK8 alone, and the addition of OA in the reaction blocked this effect (Fig. 3D, lanes 1 to 4). PP2A and PP1 were also depleted from nuclear extracts with anti-PP2A or anti-PP1 antibodies prior to CDK8 IP to exclude them from CDK8 IPs. Prior PP2A immune depletion resulted in CDK8 activity at levels similar to those observed with OA inhibition, even with the subsequent inclusion of anti-PP2A antibody in the anti-CDK8 IP (Fig. 3D, lanes 5 and 6). Assays of CDK8 IPs from PP2A- or PP1-depleted extract demonstrated a loss of the OA response after PP2A depletion but not after PP1 depletion (Fig. 3E). Figures 3D and E present kinase assays of anti-CDK8 IPs from nuclear extracts of cells expressing RV-cyclin, but similar results were obtained without RV-cyclin expression. Figure 3F shows the degree of the immune depletion of PP2A and PP1 relative to equal quantities of untreated nuclear extract. These experiments provide direct evidence for the specific PP2A activation of CDK8 during the kinase reaction. However, PR65 could not be detected in anti-CDK8 IPs by Western blotting without the inclusion of anti-PP2A antibody, and anti-PP2A IPs alone did not yield CTD phosphorylation activity *in vitro* under the conditions described (not shown).

PP2A effects on CDK8 IPs are not dependent upon other CTD kinases. CDK7, CDK8, and CDK9 target the CTD of Pol II. Anti-CDK7, anti-CDK8, and anti-CDK9 IPs were prepared from HeLa NEs with or without induced RV-cyclin expression and were assayed with or without OA for the phosphorylation of GST-CTD (Fig. 4A). CDK7 IP activity was largely unaffected by OA inhibition or RV-cyclin expression. CDK8 IPs had 21% greater CDK8 activity in the absence of OA with or without RV-cyclin expression, and RV-cyclin increased activity by 23% independently of OA. OA had nominal effects on CDK9 IP activity, and its activity was actually reduced by RV-cyclin expression (approximately 35% less with or without OA). These data demonstrate that the effects of both OA and RV-cyclin on anti-CDK8 IP activity toward the CTD are specific for CDK8 activity and are not the result of coprecipitated CDK7 or CDK9.

The probing of kinase assay blots with specific antibodies did not detect CDK8 in anti-CDK7 or anti-CDK9 IPs, and there was no detectable CDK9 in anti-CDK8 or CDK7 IPs, but small quantities of CDK7 were detectable by the Western blotting of anti-CDK8 IPs (Fig. 4B). This coprecipitated CDK7 may be responsible for a portion of the apparent CTD phosphorylation by anti-CDK8 precipitates but not for OA inhibition or RV-cyclin enhancement.

Exogenous CDK8 kinase activity is regulated by PP2A. To confirm PP2A regulation of CDK8, HeLa cells were transfected with constructs that express Flag-tagged CDK8 or a kinase-deficient CDK8 mutant (D173A) (20). The Flag-tagged CDK8 expression constructs were also cotransfected with HA-tagged RV-cyclin or HA-tagged cyclin C. Nuclear extracts from transfected cells were immune precipitated with anti-FLAG antibody and with anti-FLAG plus anti-PP2A antibodies, and the precipitates were subjected to kinase assay with GST-CTD substrate (Fig. 5). CTD phosphorylation by anti-FLAG IP was 20% greater without OA (lanes 1 and 2). The inclusion of the PP2A antibody increased FLAG-CDK8 activity and was also inhibited by OA (lanes 3 and 4). RV-cyclin expression increased activity by 37% independently of OA (lanes 1 and 5 and lanes 2 and 6). The expression of cyclin C did not enhance FLAG-CDK8 activity in the presence or absence of OA (lanes 7 and 8), and anti-FLAG IP from cells expressing the kinase-deficient mutant, D173A, had approximately half of the activity of the wild type, even with anti-PP2A antibody (lanes 9 and 10). Western analysis indicated the coprecipitation of endogenous CDK8 in the anti-FLAG IPs (not shown), which may account for the apparent activity of the kinase-deficient mutant. The results with transiently expressed, FLAG-tagged CDK8 and kinase-deficient CDK8 confirm the PP2A activation of CDK8 *in vitro* and the ability of RV-cyclin to enhance CDK8 activity in a manner not demonstrated by exogenous cyclin C.

PP2A regulates CDK8 autophosphorylation. CDK8 auto-

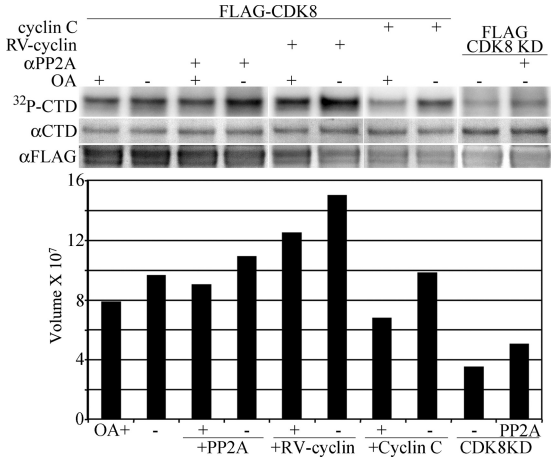

FIG 5 Exogenous FLAG-CDK8 kinase activity is regulated by PP2A and RV-cyclin. HeLa cell nuclear extracts with transiently expressed FLAG-CDK8, FLAG-CDK8 with RV-cyclin (RV-cyclin), FLAG-CDK8 with cyclin C (cyclin C), or kinase-deficient FLAG-CDK8 (FLAG-CDK8 KD) were immune precipitated with anti-FLAG antibody or with combined anti-FLAG and anti-PP2A (αPP2A) antibodies for kinase assay with GST-CTD as the substrate. Equal aliquots of washed Ab-protein G magnetic beads were suspended in a common reaction mix with or without added OA (10 nM). After incubation, GST fusion substrate was captured with added glutathione magnetic beads. IP and substrate were washed and separated by polyacrylamide gel electrophoresis and blotted onto nylon for the imaging of labeled GST-CTD substrate (^{32}P-CTD). The blot was subsequently probed with specific antibodies for the CTD (74 to 76 kDa; αCTD) and FLAG-CDK8 (56 kDa; αFLAG). The chart presents signal (relative band volume) from the phosphorimage of the CTD band.

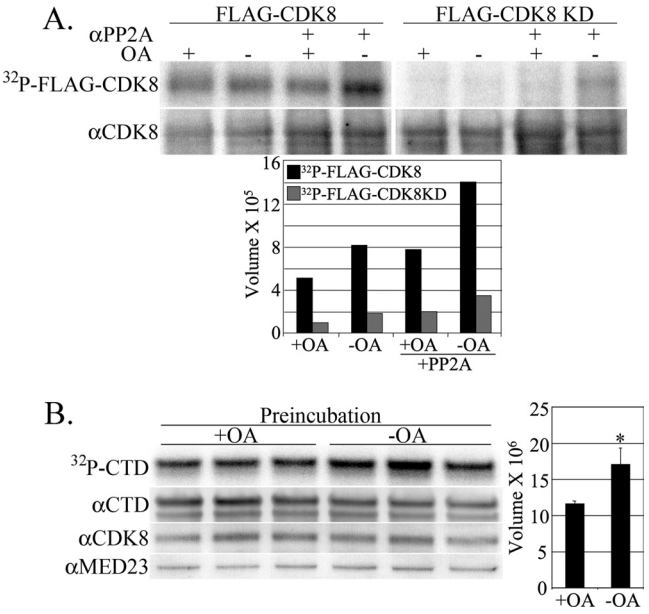

FIG 6 CDK8 autophosphorylation is regulated by PP2A. (A) HeLa cell nuclear extracts with transiently expressed FLAG-CDK8 or kinase-deficient FLAG-CDK8 (FLAG-CDK8 KD) were immune precipitated with anti-FLAG antibody or with combined anti-FLAG and anti-PP2A (αPP2A) antibodies for kinase assay with no added substrate. Equal aliquots of washed Ab-protein G magnetic beads were suspended in a common reaction mix with or without added OA (10 nM). After incubation, IPs were washed and separated by polyacrylamide gel electrophoresis and blotted onto nylon for the imaging of labeled IP proteins (56 kDa; ^{32}P-FLAG-CDK8). The single radiolabeled band was identified subsequently with anti-CDK8 Ab (αCDK8). The chart presents signal (relative band volume) from the phosphorimage of the FLAG-CDK8 band. (B) Anti-CDK8 IPs from HeLa cell nuclear extracts were assayed in triplicate reactions. Equal aliquots of washed CDK8 Ab-protein G magnetic beads were preincubated in a common reaction mix with or without added OA (20 nM) for 50 min prior to the addition of a single mix with GST-CTD substrate, [γ^{32}P]ATP, and excess OA (100 nM) to both reactions. After further incubation, GST-CTD was captured with added glutathione magnetic beads. IP and substrate were washed and separated by polyacrylamide gel electrophoresis and blotted onto nylon for the imaging of labeled GST-CTD substrate (^{32}P-CTD). Blots were subsequently probed with specific antibodies for the CTD (74 to 76 kDa; αCTD), CDK8 (53 kDa; αCDK8), and MED23 (140 kDa; αMED23). The chart presents signal (relative band volume) from the phosphorimage of the CTD band. The asterisk indicates statistical significance associated with preincubation with OA ($P < 0.01$).

phosphorylation was first identified by Gold et al. (20) and subsequently shown to be requisite for the CDK8 phosphorylation of the CTD by recombinant CDK8 complexes (26). Anti-FLAG IPs from nuclear extracts of cells transfected with FLAG-CDK8 or kinase-deficient FLAG-CDK8 expression vectors were subjected to kinase assays with no added substrate (Fig. 6A). The phosphorimaging of the assay blot demonstrated the *in vitro* phosphorylation of an immune-precipitated protein the size of FLAG-CDK8, and OA reduced the phosphorylation of this protein by 47% (lanes 1 and 2). The inclusion of anti-PP2A antibody in the IP increased activity by 43% in the absence of OA (lanes 2 and 4). The identity of the labeled band as FLAG-tagged CDK8 was confirmed with anti-CDK8 antibody (Fig. 6A, bottom). The phosphorylation of the kinase-deficient FLAG-CDK8 was very low, indicating that a functional CDK8 kinase domain was required for the observed phosphorylation (lanes 5 to 8 and gray bars). The results demonstrate that a PP2A-mediated dephosphorylation reaction precedes CDK8 autophosphorylation and activation.

This proposed temporal role for PP2A action prior to CDK8 activation by autophosphorylation was tested by the preincubation of anti-CDK8 IPs in kinase buffer with or without OA. After allowing dephosphorylation to occur *in vitro*, the IPs were assayed for the phosphorylation of the CTD substrate in the presence of OA by the addition of a common reaction mixture containing GST-CTD, [γ-^{32}P]ATP, and excess OA (100 nM). The preactivation of CDK8 without OA was sufficient for a subsequent 32% increase in CTD phosphorylation in the presence of OA (Fig. 6B).

PP2A activation does not extend to histone H3 phosphorylation. Serine 10 (S10) of histone H3 is also a CDK8 substrate, whether the kinase is present in the free CDK8 submodule or in the Mediator complex (27). Anti-CDK8 IPs include both CDK8 complexes. The inclusion of recombinant histone H3 as a substrate, along with GST-CTD, recapitulated the increase in CDK8 activity associated with RV-cyclin expression: CDK8 phosphorylation of histone H3 was doubled (Fig. 7) ($P < 0.001$). However, the addition of OA to the kinase reactions had no significant effect on histone H3 phosphorylation in the presence or absence of RV-cyclin expression (Fig. 7). CTD phosphorylation in these same reactions remained susceptible to OA inhibition (Fig. 3A). This result demonstrates a consistent effect of RV-cyclin on CDK8 activity, but it also indicates the specific PP2A regulation of CTD phosphorylation and not of histone H3 phosphorylation *in vitro*. This may reflect two subsets of CDK8: one that preferentially phosphorylates histone H3 *in vitro*, such as CDK8 in the submodule, versus a CDK8 subset that phosphorylates the CTD, such as CDK8 in the Mediator complex.

Figure 8 presents a model of RV-cyclin regulation of CDK8

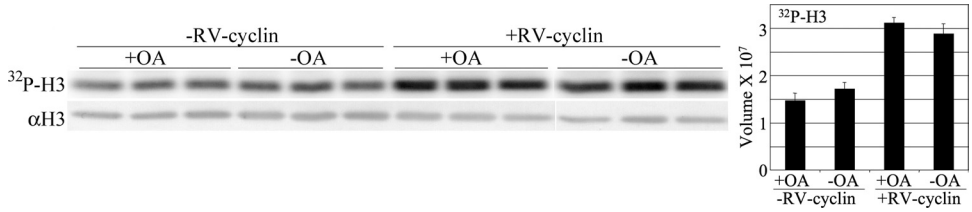

FIG 7 RV-cyclin enhances, but okadaic acid (OA) does not inhibit, histone H3 phosphorylation. Anti-CDK8 IPs from nuclear extracts of matched uninduced (−RV-cyclin) and induced (+RV-cyclin) HeLa cells were assayed in triplicate reactions. Equal aliquots of washed CDK8 Ab-protein G magnetic beads were suspended in a common reaction mix containing recombinant mouse histone H3 and GST-CTD as substrates and with or without added OA (10 nM). After incubation, histone H3 substrate was captured with specific antibody and additional protein G magnetic beads and GST-CTD with glutathione magnetic beads. IP and substrates were washed and separated by polyacrylamide gel electrophoresis and blotted onto nylon for the imaging of labeled histone H3 substrate (^{32}P-H3) (Fig. 3A, CTD). The blot was subsequently probed with specific antibody for histone H3 (17 kDa; αH3). The chart presents means and standard deviations of signal (relative band volume) from the phosphorimage of the H3 band.

activity, both by the direct activation of kinase function and possibly through its interaction with the A subunit of PP2A. CDK8 in the free submodule or in CDK8-Mediator is subject to RV-cyclin binding and increased kinase activity toward histone H3 and CTD substrates compared to cyclin C. In addition, CDK8-Mediator is further subject to dephosphorylation by PP2A, which triggers autophosphorylation and full kinase activity toward the CTD (*in vitro*). RV-cyclin might enhance this CDK8 activation process as well by colocalizing PP2A and its CDK8 substrate. Its specific targeting of transcription initiation complexes via TAF9 (47) could stabilize such interactions.

DISCUSSION

The dysregulation of CDK8 function is clearly associated with the development of cancer (16, 25, 34, 35). In melanoma, the loss of expression of the histone variant macro-H2A results in the upregulation of CDK8 expression, and this correlates with increasing malignancy (25). In colorectal cancer, CDK8 expression is frequently increased by *CDK8* gene amplification (52% of cases [16]). Colon cancer cell lines remain dependent upon elevated CDK8 expression for growth, and the overexpression of functional CDK8 can transform cells *in vitro*. The increases of CDK8 levels in disease are not large; colon cancer cell lines typically have one to three additional copies of the gene encoding CDK8, suggesting that as little as two to three times the normal level of CDK8 activity is oncogenic. In osteosarcoma, the gene encoding cyclin C is frequently lost, and cell lines derived from these tumors are dependent upon continued cyclin C depletion for growth (35). This association of cyclin C depletion with cancer points to a possible role as a governor of CDK8 activity. Any dysregulation of CDK8 activity, whether by the loss of control or modest increase in total kinase activity, may be oncogenic. We suggest that the functional increase in CDK8 enzyme activity that is associated with RV-cyclin emulates the level of CDK8 activity associated with disease. This hypothesis is borne out by very large increases in the expression of specific host genes when RV-cyclin is expressed (9).

The enzymatic activity of cyclin-dependent kinases is regulated by reversible phosphorylation. Phosphatases may serve as positive or negative regulators. The activity of most CDKs is dependent upon binding to a cyclin followed by phosphorylation within the activation loop (T loop). The phosphorylated residue in the T loop then interacts with three conserved arginines, which induces a conformational change allowing substrate access to the ATP binding site. An example is CDK9, which binds cyclin T and is a

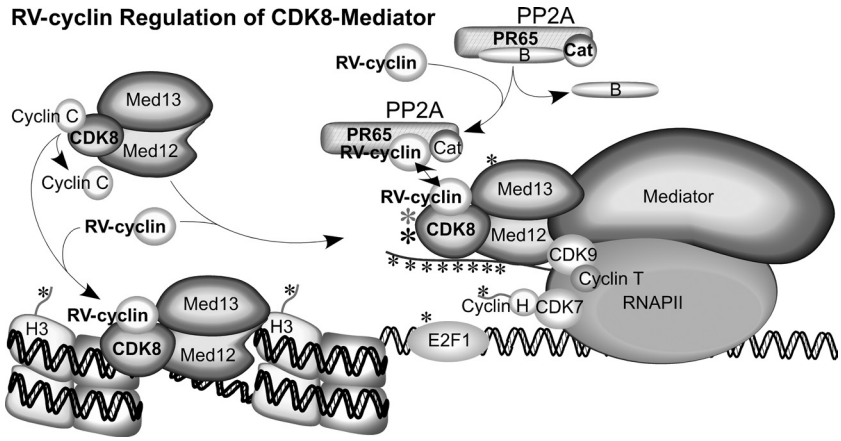

FIG 8 Proposed model of RV-cyclin regulation of CDK8 activity. RV-cyclin displaces cyclin C from CDK8 in the submodule and in CDK8-Mediator complexes associated with RNA Pol II and transcription complexes. CDK8 has greater enzymatic activity with RV-cyclin than cyclin C binding. CDK8-Mediator is also subject to dephosphorylation by PP2A, which triggers autophosphorylation and full kinase activity toward the CTD of RNA Pol II. This mechanism functions with or without RV-cyclin. RV-cyclin also binds the PP2A scaffold subunit, PR65, and excludes the regulatory B subunit. RV-cyclin may increase the PP2A-CDK8 activation process by colocalizing PP2A with its CDK8 substrate at active transcription sites. Known CDK8 substrates, histone H3, RNA Pol II CTD, E2F1, cyclin H, Med13, and CDK8 itself, are illustrated with asterisks.

component of the transcription elongation complex, P-TEFb. The CDK9 T loop (T186) can be autophosphorylated to form an active kinase that localizes to nuclear speckles where the further exchange of negative and positive regulatory components occurs (14, 56). CDK9 kinase activity is also positively regulated by the PP1 dephosphorylation of residue S175, a reaction that contributes to the activation of HIV-1 transcription (3).

The control of CDK8 activity remains poorly understood. Hoeppner et al. determined the crystal structure of cyclin C (SRB11) from *Schizosaccharomyces pombe* (23), and the modeling of a CDK8/cyclin C complex suggested that CDK8 was not phosphorylated in the activation loop. They proposed that the activation of CDK8 is the result of an interaction of an exposed glutamate residue in cyclin C with three arginine residues in the activation loop to induce an open conformation of the CDK8 ATP-binding site. This model is supported by the recently solved crystal structure of human CDK8/cyclin C in a complex with sorafenib, an anticancer drug that binds to the catalytic cleft of CDK8 (50). These studies revealed that the CDK8 activation loop does not contain a phosphoresidue and supports the cyclin C model described by Hoeppner et al. (23). This is in contrast to a computational study of CDK8 structure, which predicted that a threonine residue near the CDK8 activation loop is phosphorylated (57). To date, only two phosphorylation sites have been physically identified, and they are located in the C terminus of CDK8 (T410 and S413) (36), which is distant from the activation segment (50). These or other putative kinase targets could regulate the activation loop.

The sequence alignment of RV-cyclin and cyclin C revealed a number of conserved residues that are critical for binding to CDK8. Mutation of two of these residues in RV-cyclin ($K80^{RV\text{-}Cyc}$/$K96^{CycC}$ and $E111^{RV\text{-}Cyc}$/$E139^{CycC}$) disrupts RV-cyclin binding to CDK8 (9). The exposed glutamate residues in yeast (E91) and human cyclin C (E99) that interact with the arginine residues in the CDK8 activation loop also align with RV-cyclin E83, suggesting that RV-cyclin has the capacity to bind CDK8 and yield an active conformation in the CDK8 T loop. The data presented here support direct action by the RV-cyclin on CDK8 structure to enhance its activity compared to that of exogenous cyclin C (Fig. 5). The model in Fig. 8 includes this direct aspect of the RV-cyclin regulation of CDK8-Mediator.

The RV-cyclin enhancement of CDK8-dependent RNA Pol II CTD phosphorylation *in vitro* may result from the formation of an open conformation of the CDK8 active site. The CDK8 immune precipitate in this case is likely to be a component of the Mediator complex, since the endogenous CDK8 submodule is unable to phosphorylate the CTD *in vitro*, and approximately 70% of the CDK8 in HeLa nuclear extracts are part of the Mediator complex (27). Also, Med23, a component of CDK8-Mediator, was present in the anti-CDK8 IPs (Fig. 1, 3A, and 6B). This result places RV-cyclin at transcription complexes where CDK8 phosphorylates and activates RNA Pol II and promotes transcription elongation through the recruitment of CDK9 (13). We hypothesize that the contribution of RV-cyclin to transcription elongation processivity is an important part of its ability to significantly enhance the expression of a number of cell cycle regulatory genes, specifically the known oncogene *cyclin D1* (9) and immediate-early genes *FOS* and *EGR1* (C. Birkenheuer, S. L. Quackenbush, and J. Rovnak, unpublished data). The transcription elongation of *FOS* and *EGR1* during serum response is positively regulated by CDK8 (13, 53). The RV-cyclin stabilization of CDK8 in an active conformation may contribute directly to the increased expression of these regulators of cell proliferation and promote tumorigenesis.

RV-cyclin also binds the Aα subunit of PP2A. This led to the finding that CDK8 kinase activity is regulated by PP2A. The anti-CDK8 IPs are at least partially phosphorylated at a site that serves as both a substrate for PP2A phosphatase activity and as a regulator of CDK8 autophosphorylation and subsequent CTD phosphorylation. What is the role for PP2A in the context of its RV-cyclin interaction? The avidity of the RV-cyclin for the nuclear compartment and, specifically, for IGCs and perichromatin fibrils has been well established (43, 44, 46). The enrichment of a variety of transcription components in these nuclear regions, including CDK8, CDK9, and hyperphosphorylated forms of RNA Pol II, has also been shown (5, 14, 22, 46, 51). An ability of the RV-cyclin to deliver additional, active PP2A to IGCs may promote CDK8 function by dephosphorylation. The RV-cyclin may also stabilize PP2A specifically at active transcription complexes that include CDK8-Mediator. The transcription activation domain in the carboxy terminus of RV-cyclin directly binds TAF9 at these sites (47). The interaction of this separate domain may juxtapose PP2A and CDK8-Mediator. The data presented here do not specifically support the PP2A-dependent RV-cyclin activation of CDK8, but they do not preclude such a mechanism.

Each PP2A heterotrimer contains a specific B subunit that functions in both its localization and substrate specificity (recently reviewed by Eichhorn et al. [15]). Regions of the B subunit interact directly with positively charged motifs adjacent to targeted phosphoepitopes to stabilize contacts by the catalytic subunit. Among the four families of PP2A B subunits, the B′ family (B56 or PR61) is comprised of types α, β, ε, δ, and γ (15, 59). Five isoforms of B56γ have been identified, isoforms 1, 2, and 3 have been observed in the nucleus, and γ1 is concentrated in IGCs (18). We hypothesize a role for the PP2A B56γ1 isoform in the regulation of CDK8. In this context, the RV-cyclin displacement of the B subunit that normally targets CDK8 would also require the RV-cyclin replacement of the function of that B subunit for localization and substrate recognition. Although RV-cyclin could serve to localize PP2A at CDK8-Mediator, its ability to provide substrate recognition is unclear.

The anti-CDK8 IPs tested here contain the proportions of CDK8 subpopulations observed previously: approximately 30% as free submodule and 70% in Mediator complex (27). Either form should be capable of phosphorylating the recombinant H3 substrate *in vitro*, but only CDK8-Mediator phosphorylates the CTD. RV-cyclin enhanced the phosphorylation of both histone H3 (Fig. 7) and GST-CTD by anti-CDK8 IPs (Fig. 1, 3, 4, and 5), but only CTD phosphorylation was subject to inhibition by okadaic acid. This difference in PP2A response suggests that the RV-cyclin enhancement of histone H3 phosphorylation by CDK8 occurs via a direct, PP2A-independent mechanism and supports the conclusion that the additive enhancement of CTD phosphorylation also results from direct RV-cyclin action. Furthermore, OA inhibition specifically of CTD phosphorylation suggests that CDK8-Mediator is the primary target for dephosphorylation by PP2A *in vitro*. However, the loss of PP2A regulation *in vitro* may only indicate the prior, complete PP2A dephosphorylation of CDK8 in the submodule *in vivo* or a lack of sufficient PP2A associated with the submodule in the CDK8 IP. Either way, the CDK8

complexes that are subject to PP2A regulation now can be separated based on their substrate specificity and OA sensitivity.

We have identified a role for RV-cyclin in the enhancement of CDK8 activity and a PP2A-mediated mechanism for CDK8 activation by dephosphorylation prior to CDK8 autophosphorylation. The specific phosphoepitope(s) that serves as CDK8 regulator and PP2A substrate remains unknown. It is clear that the anti-CDK8 immune precipitate contains many bound proteins, including components of the Mediator complex and RNA Pol II (45, 46). Likely candidates for PP2A dephosphorylation include CDK8 itself and Med13, which binds to and is phosphorylated by CDK8 (26). Cyclin C controls the structure of the CDK8 active site and also has many predicted serine/threonine phosphorylation sites that may be dephosphorylated by PP2A.

ACKNOWLEDGMENTS

We thank Teri McLain, Director, Protein Expression Facility, Department of Biochemistry and Molecular Biology, Colorado State University, for the generous gift of mouse histone H3 and Scott Carver and Forrest Ackart for assistance with statistical analysis.

This research was supported in part by American Cancer Society grant RPG-00313-01-MBC to S.L.Q. and National Institutes of Health grant RO1CA95056 from the National Cancer Institute.

The content is solely the responsibility of the authors and does not necessarily represent the official views of the National Cancer Institute or the National Institutes of Health.

REFERENCES

1. **Akoulitchev S, Chuikov S, Reinberg D.** 2000. TFIIH is negatively regulated by cdk8-containing mediator complexes. Nature **407**:102–106.
2. **Alarcon C, et al.** 2009. Nuclear CDKs drive Smad transcriptional activation and turnover in BMP and TGF-beta pathways. Cell **139**:757–769.
3. **Ammosova T, et al.** 2011. Protein phosphatase-1 activates CDK9 by dephosphorylating Ser175. PLoS One **6**:1–13.
4. **Aragon E, et al.** 2011. A Smad action turnover switch operated by WW domain readers of a phosphoserine code. Genes Dev. **25**:1275–1288.
5. **Bex F, McDowall A, Burny A, Gaynor R.** 1997. The human T-cell leukemia virus type 1 transactivator protein Tax colocalizes in unique nuclear structures with NF-kB proteins. J. Virol. **71**:3484–3497.
6. **Bowser PR, Wolfe MJ, Forney JL, Wooster GA.** 1988. Seasonal prevalence of skin tumors from walleye (Stizostedion vitreum) from Oneida Lake, New York. J. Wildlife Dis. **24**:292–298.
7. **Bowser PR, Wooster GA.** 1991. Regression of dermal sarcoma in adult walleyes (Stizostedion vitreum). J. Aquat. Anim. Health **3**:147–150.
8. **Bowser PR, Wooster GA, Quackenbush SL, Casey RN, Casey JW.** 1996. Comparison of fall and spring tumors as inocula for experimental transmission of walleye dermal sarcoma. J. Aquat. Anim. Health **8**:78–81.
9. **Brewster C, Birkenheuer C, Vogt M, Quackenbush S, Rovnak J.** 2011. The retroviral cyclin of walleye dermal sarcoma virus binds cyclin-dependent kinases 3 and 8. Virology **409**:299–307.
10. **Chen W, et al.** 2004. Identification of specific PP2A complexes involved in human cell transformation. Cancer Cell **5**:127–136.
11. **Conaway RC, Conaway JW.** 2011. Function and regulation of the Mediator complex. Curr. Opin. Genet. Dev. **21**:225–230.
12. **Dignam JD, Lebovitz RM, Roeder RG.** 1983. Accurate transcription initiation by RNA polymerase II in a soluble extract from isolated mammalian nuclei. Nucleic Acids Res. **11**:1475–1489.
13. **Donner AJ, Ebmeier CC, Taatjes DJ, Espinosa JM.** 2010. CDK8 is a positive regulator of transcriptional elongation within the serum response network. Nat. Struct. Mol. Biol. **17**:194–201.
14. **Dow EC, Liu H, Rice AP.** 2010. T-loop phosphorylated Cdk9 localizes to nuclear speckle domains which may serve as sites of active P-TEFb function and exchange between the Brd4 and 7SK/HEXIM1 regulatory complexes. J. Cell. Physiol. **224**:84–93.
15. **Eichhorn P, Creyghton M, Bernards R.** 2009. Protein phosphatase 2A regulatory subunits and cancer. Biochim. Biophys. Acta **1795**:1–15.
16. **Firestein R, et al.** 2008. CDK8 is a colorectal cancer oncogene that regulates beta-catenin activity. Nature **455**:547–551.
17. **Galbraith M, Donner A, Espinosa J.** 2010. CDK8: a positive regulator of transcription. Transcription **1**:4–12.
18. **Gigena M, Ito A, Nojima H, Rogers T.** 2005. A B56 regulatory subunit of protein phosphatase 2A localizes to nuclear speckles in cardiomyocytes. Am. J. Physiol. Heart Circ. Physiol. **289**:H285–H294.
19. **Gold MO, Rice AP.** 1998. Targeting of CDK8 to a promoter-proximal RNA element demonstrates catalysis-dependent activation of gene expression. Nucleic Acids Res. **26**:3784–3788.
20. **Gold MO, Tassan JP, Nigg EA, Rice AP, Herrmann CH.** 1996. Viral transactivators E1A and VP16 interact with a large complex that is associated with CTD kinase activity and contains CDK8. Nucleic Acids Res. **24**:3771–3777.
21. **Groves MR, Hanlon N, Turowski P, Hemmings BA, Barford D.** 1999. The structure of the protein phosphatase 2A PR65/A subunit reveals the conformation of its 15 tandemly repeated HEAT motifs. Cell **96**:99–110.
22. **Herrmann CH, Mancini MA.** 2001. The Cdk9 and cyclin T subunits of TAK/P-TEFb localize to splicing factor-rich nuclear speckle regions. J. Cell Sci. **114**:1491–1503.
23. **Hoeppner S, Baumli S, Cramer P.** 2005. Structure of the mediator subunit cyclin C and its implications for CDK8 function. J. Mol. Biol. **350**:833–842.
24. **Ishihara H, et al.** 1989. Calyculin A and okadaic acid: inhibitors of protein phosphatase activity. Biochem. Biophys. Res. Commun. **159**:871–877.
25. **Kapoor A, et al.** 2010. The histone variant macroH2A suppresses melanoma progression through regulation of CDK8. Nature **468**:1105–1109.
26. **Knuesel MT, Meyer KD, Bernecky C, Taatjes DJ.** 2009. The human CDK8 subcomplex is a molecular switch that controls Mediator coactivator function. Genes Dev. **23**:439–451.
27. **Knuesel MT, Meyer KD, Donner AJ, Espinosa JM, Taatjes DJ.** 2009. The human CDK8 subcomplex is a histone kinase that requires Med12 for activity and can function independently of mediator. Mol. Cell. Biol. **29**:650–661.
28. **Kremmer E, Ohst K, Kiefer J, Brewis N, Walter G.** 1997. Separation of PP2A core enzyme and holoenzyme with monoclonal antibodies against the regulatory A subunit: abundant expression of both forms in cells. Mol. Cell. Biol. **17**:1692–1701.
29. **LaPierre LA, Casey JW, Holzschu DL.** 1998. Walleye retroviruses associated with skin tumors and hyperplasias encode cyclin D homologs. J. Virol. **72**:8765–8771.
30. **Martin ES, et al.** 2007. Common and distinct genomic events in sporadic colorectal cancer and diverse cancer types. Cancer Res. **67**:10736–10743.
31. **Martineau D, Bowser PR, Renshaw PR, Casey JW.** 1992. Molecular characterization of a unique retrovirus associated with a fish tumor. J. Virol. **66**:596–599.
32. **Martineau D, Renshaw R, Williams JR, Casey JW, Bowser PR.** 1991. A large unintegrated retrovirus DNA species present in a dermal tumor of walleye Stizostedion vitreum. Dis. Aquat. Organisms **10**:153–158.
33. **Meyer KD, et al.** 2008. Cooperative activity of cdk8 and GCN5L within Mediator directs tandem phosphoacetylation of histone H3. EMBO J. **27**:1447–1457.
34. **Morris EJ, et al.** 2008. E2F1 represses beta-catenin transcription and is antagonized by both pRB and CDK8. Nature **455**:552–556.
35. **Ohata N, et al.** 2006. Highly frequent allelic loss of chromosome 6q16-23 in osteosarcoma: involvement of cyclin C in osteosarcoma. Int. J. Mol. Med. **18**:1153–1158.
36. **Oppermann F, et al.** 2009. Large-scale proteomics analysis of the human kinome. Mol. Cell Proteomics **8**:1751–1764.
37. **Pallas DC, et al.** 1990. Polyoma small and middle T antigens and SV40 small t antigen form stable complexes with protein phosphatase 2A. Cell **60**:167–176.
38. **Pallas DC, et al.** 1992. The third subunit of protein phosphatase 2A (PP2A), a 55-kilodalton protein which is apparently substituted for by T antigens in complexes with the 36- and 63-kilodalton PP2A subunits, bears little resemblance to T antigens. J. Virol. **66**:886–893.
39. **Quackenbush SL, Holzschu DL, Bowser PR, Casey JW.** 1997. Transcriptional analysis of walleye dermal sarcoma virus (WDSV). Virology **237**:107–112.
40. **Quackenbush SL, Linton A, Brewster CD, Rovnak J.** 2009. Walleye dermal sarcoma virus rv-cyclin inhibits NF-κB-dependent transcription. Virology **386**:55–60.

41. **Rickert P, Corden JL, Lees E.** 1999. Cyclin C/CDK8 and cyclin H/CDK7/p36 are biochemically distinct CTD kinases. Oncogene **18**:1093–1102.
42. **Rickert P, Seghezzi W, Shanahan F, Cho H, Lees E.** 1996. Cyclin C/CDK8 is a novel CTD kinase associated with RNA polymerase II. Oncogene **12**:2631–2640.
43. **Rovnak J, Casey JW, Quackenbush SL.** 2001. Intracellular targeting of walleye dermal sarcoma virus Orf A (rv-cyclin). Virology **280**:31–40.
44. **Rovnak J, Casey RN, Brewster CD, Casey JW, Quackenbush SL.** 2007. Establishment of productively infected walleye dermal sarcoma explant cells J. Gen. Virol. **88**:2583–2589.
45. **Rovnak J, Hronek BW, Ryan SO, Cai S, Quackenbush SL.** 2005. An activation domain within the walleye dermal sarcoma virus retroviral cyclin protein is essential for inhibition of the viral promoter. Virology **342**:240–251.
46. **Rovnak J, Quackenbush SL.** 2002. Walleye dermal sarcoma virus cyclin interacts with components of the Mediator complex and the RNA polymerase II holoenzyme. J. Virol. **76**:8031–8039.
47. **Rovnak J, Quackenbush SL.** 2006. Walleye dermal sarcoma virus retroviral cyclin directly contacts TAF9. J. Virol. **80**:12041–12048.
48. **Ruediger R, Hentz M, Fait J, Mumby M, Walter G.** 1994. Molecular model of the A subunit of protein phosphatase 2A: interaction with other subunits and tumor antigens. J. Virol. **68**:123–129.
49. **Sablina A, Hector M, Colpaert N, Hahn W.** 2010. Identification of PP2A complexes and pathways involved in cell transformation. Cancer Res. **70**:10474–10484.
50. **Schneider E, et al.** 2011. The structure of CDK8/CycC implicates specificity in the CDK/Cyclin family and reveals interaction with a deep-pocket binder. J. Mol. Biol. **412**:251–266.
51. **Semmes OJ, Jeang K-T.** 1996. Localization of human T-cell leukemia virus type 1 Tax to subnuclear compartments that overlap with interchromatin speckles. J. Virol. **70**:6347–6357.
52. **Sontag E, et al.** 1993. The interaction of SV40 small tumor antigen with protein phosphatase 2A stimulates the Map kinase pathway and induces cell proliferation. Cell **75**:887–897.
53. **Stevens JL, Cantin GT, Wang G, Shevchenko A, Berk AJ.** 2002. Transcription control by E1A and MAP kinase pathway via Sur2 mediator subunit. Science **296**:755–758.
54. **Tsafrir D, et al.** 2006. Relationship of gene expression and chromosomal abnormalities in colorectal cancer. Cancer Res. **66**:2129–2137.
55. **Ulug ET, Cartwright AJ, Coutneidge SA.** 1992. Characterization of the interaction of polyomavirus middle T antigen with type 2A protein phosphatase. J. Virol. **66**:1458–1467.
56. **Wang Y, et al.** 2008. Phosphatase PPM1A regulates phosphorylation of Thr-186 in the Cdk9 T-loop. J. Biol. Chem. **283**:33578–33584.
57. **Xu W, Ji JY.** 2011. Dysregulation of CDK8 and Cyclin C in tumorigenesis. J. Genet. Genomics **38**:439–452.
58. **Yamamoto T, MacDonald RD, Gillespie DC, Kelly RK.** 1976. Viruses associated with lymphocystis and dermal sarcoma of walleye (Stizostedion vitreum vitreum). J. Fish Res. Board Canada **33**:2408–2419.
59. **Yang J, Phiel C.** 2010. Functions of B56-containing PP2As in major developmental and cancer signaling pathways. Life Sci. **87**:659–666.
60. **Zhang Z, Martineau D.** 1999. Walleye dermal sarcoma virus: OrfA N-terminal end inhibits the activity of a reporter gene directed by eukaryotic promoters and has a negative effect on the growth of fish and mammalian cells. J. Virol. **73**:8884–8889.